Monte Carlo Shell Model Towards Ab Initio Calculations

T. Abe[a], P. Maris[b], T. Otsuka[a,c,d], N. Shimizu[c], Y. Tsunoda[a], Y. Utsuno[e] and J. P. Vary[b]

[a] *Department of Physics, the University of Tokyo, Hongo, Tokyo 113-0033, Japan*
[b] *Department of Physics and Astronomy, Iowa State University, Ames, IA 50011, USA*
[c] *Center for Nuclear Study, the University of Tokyo, Hongo, Tokyo 113-0033, Japan*
[d] *National Superconducting Cyclotron Laboratory, Michigan State University, East Lansing, MI 48824, USA*
[e] *Advanced Science Research Center, Japan Atomic Energy Agency, Tokai, Ibaraki 319-1195, Japan*

Abstract

We report on our recent application of the Monte Carlo Shell Model (MCSM) to no-core calculations. After the brief introduction, the performance of the MCSM on the K computer is discussed. At the initial stage of the application, we have performed benchmark calculations in the p-shell region. Results are compared with those in the Full Configuration Interaction and No-Core Full Configuration methods. These are found to be consistent with each other within quoted uncertainties when they could be quantified. The preliminary results in $N_{\rm shell} = 5$ reveal the onset of systematic convergence pattern.

Keywords: *Monte Carlo Shell Model; No-Core Shell Model; ab initio approach*

1 Introduction

One of the major challenges in nuclear theory is to reproduce and to predict nuclear structure and reactions from *ab initio* calculations with realistic nuclear forces. Among the *ab initio* nuclear many-body approaches for $A \geq 4$ [1], the No-Core Shell Model (NCSM) is one of the powerful methods for the study of nuclear structure and reactions in the p-shell nuclei [2].

As the NCSM treats all the nucleons on an equal footing, computational demands for the calculations explode exponentially as the number of nucleons increases. Current computational resources limit the direct diagonalization of the Hamiltonian matrix using the Lanczos algorithm to basis spaces with a dimension of around 10^{10}. Shell-model calculations in the $N_{\rm shell}$ truncation is limited in the lower p-shell region (Fig. 1). In order to access heavier nuclei beyond the p-shell region with larger basis dimensions, many efforts have been devoted to the NCSM calculations. One of these approaches is the Importance–Truncated NCSM (IT-NCSM) [3] where the basis spaces are extended by using an importance measure evaluated using perturbation theory. Another approach is the Symmetry–Adapted NCSM (SA-NCSM) [4] where the basis spaces are truncated by the selected symmetry groups. Similar to these attempts, the Monte Carlo NCSM (MC-NCSM) [5, 6] is one of the promising candidates to go beyond the Full Configuration Interaction (FCI) method which is a different truncation of the basis states that commonly used in the NCSM. Shell-model

Proceedings of International Conference 'Nuclear Theory in the Supercomputing Era — 2013' (NTSE-2013), Ames, IA, USA, May 13–17, 2013. Eds. A. M. Shirokov and A. I. Mazur. Pacific National University, Khabarovsk, Russia, 2014, p. 294.
http://www.ntse-2013.khb.ru/Proc/Abe.pdf.

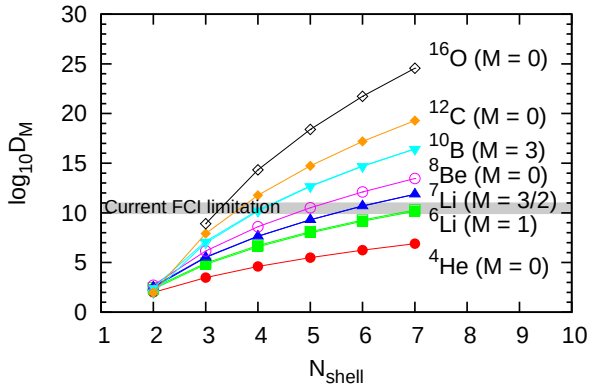

Figure 1: M-scheme dimension for light nuclei as a function of basis space cutoff, $N_{\rm shell}$.

calculations with an assumed inert core by the MCSM have succeeded in obtaining the approximated solutions where the direct diagonalization is difficult due to large dimensionalities as described in Fig. 2.

In these proceedings, we focus on the latest application of the MCSM toward the *ab initio* no-core calculations, which has become feasible recently with the aid of the major developments in the MCSM algorithm [7] and also a remarkable growth in the computational power of the state-of-the-art supercomputers, such as the K computer. Most of the benchmark results in the MC-NCSM presented here are summarized in Ref. [6].

2 Monte Carlo Shell Model

2.1 Brief overview

The MCSM has been developed mainly for conventional shell-model calculations with an assumed inert core [8]. Recently the algorithm and code itself have been heavily revised and rewritten so as to accommodate massively parallel computing environments [7]. Now we can apply the MCSM not only to conventional shell-model

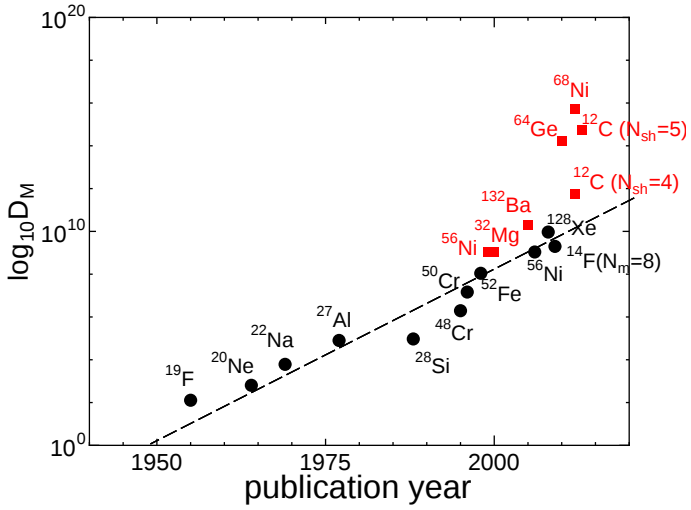

Figure 2: M-scheme dimension for conventional shell-model calculations with an assumed inert core as a function of publication year (right). Red squares are for the MCSM results, and black circles are for the conventional shell-model results by the direct diagonalization with the Lanczos technique.

calculations but also to no-core calculations.

The MCSM approach proceeds through a sequence of diagonalization steps within the Hilbert subspace spanned by the deformed Slater determinants in the HO single-particle basis. The many-body basis state $|\Psi^{J^\pi M}\rangle$ is approximated as a linear combination of non-orthogonal angular-momentum (J) and parity (π) projected deformed Slater determinants with good total angular momentum projection (M),

$$|\Psi^{J^\pi M}\rangle = \sum_{n=1}^{N_b} f_n \sum_{K=-J}^{J} g_{nK}\, P^J_{MK}\, P^\pi |\phi_n\rangle, \tag{1}$$

where N_b is the number of Slater determinants. P^J_{MK} is the projection operator for the total angular momentum J with its z-projection in the laboratory (body-fixed) frame, M (K). P^π is the projection operator for the parity. The coefficients f and g are determined by the diagonalization of Hamiltonian matrix. The deformed Slater determinant $|\phi\rangle$ in Eq. (1) is described as

$$|\phi\rangle = \prod_{i=1}^{A} a_i^\dagger |-\rangle, \tag{2}$$

with the vacuum $|-\rangle$ and the creation operator, $a_i^\dagger = \sum_{\alpha=1}^{N_{\rm sp}} c_\alpha^\dagger\, D_{\alpha i}$. $N_{\rm sp}$ is specified by the cutoff of the single particle basis space, $N_{\rm shell}$. The transformation coefficients D form the complex $N_{\rm sp} \times A$ matrix with the normalization condition, $D^\dagger D = 1$. Importance-truncated bases $|\phi\rangle$ are stochastically sampled so as to minimize the energy variationally. With increasing the number of importance-truncated basis states, the computed energy converges from above to the exact value and gives the variational upper bound. An exploratory no-core MCSM investigation of the proof-of-principle type has been done for the low-lying states of the Be isotopes by applying the existing MCSM algorithm with a core to a no-core problem [5].

Recent improvements on the MCSM algorithm have enabled significantly larger calculations [7]. The crucial developments for no-core calculations achieve (1) the efficient computation of matrix products for the most time-consuming part in the MCSM calculations, (2) the conjugate gradient method in the basis-search process, and (3) the energy-variance extrapolation for our MCSM (approximated) results into the FCI (exact) ones in the finite basis spaces. Because of space limitations, we refer for the details of these improvements to Ref. [7].

As a typical example of the implementation, the behavior of the ground-state energies of ^{4}He (0^+) and ^{12}C (0^+) with respect to the number of basis states and to the energy variance are shown in Fig. 3. From Fig. 3, one can see that the MCSM results can be extrapolated into the FCI ones by using the quadratic fit function with respect to the energy variance ΔE_2 of $E(\Delta E_2) = E(\Delta E_2 = 0) + c_1 \Delta E_2 + c_2 (\Delta E_2)^2$ with the fit parameters, $E(\Delta E_2 = 0)$, c_1, and c_2.

2.2 Tests on the K computer

At the initial stage of the implementation of K computer, we have performed some test calculations to measure our code performance. In this subsection, we show some of the test calculations: the ratio to the peak performance and the parallel efficiency of our code.

In order to measure our code performance on K computer, we have chosen the optimization of 15th basis dimension of the wave function in $N_{\rm shell} = 5$ with 100 CG iterations without the preprocessing as a test case. The code has run on K computer by using MPI/OpenMP with 8 threads.

Figure 4 illustrate our recent MCSM code performance. The left panel of Fig. 4 shows the ratio to the peak performance in the calculation of the ^{4}He 0^+ ground

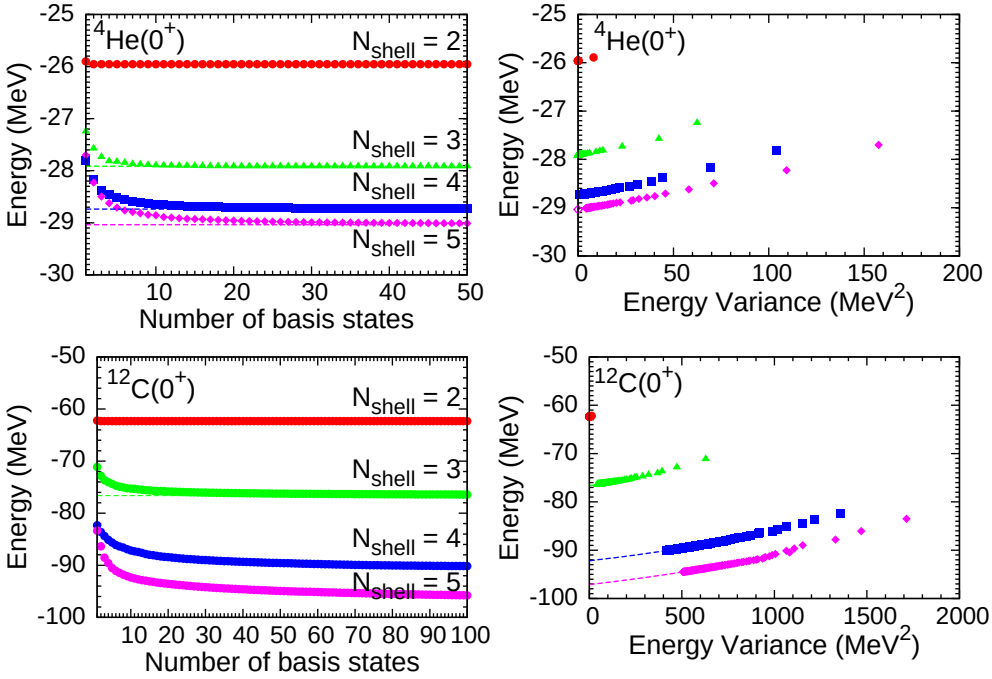

Figure 3: ^{4}He and ^{12}C 0^+ ground-state energies as functions of number of basis states (left) and energy variance (right). From the above to the bottom, the symbols (horizontal dashed lines in the left figure and open symbols at the zero energy variance in the right figure) are the MCSM (FCI) results in $N_{\rm shell} = 2$, 3, 4 and 5, respectively. Note that the results of ^{12}C in $N_{\rm shell} = 4$ and 5 are obtained only by the MCSM. See Ref. [6] for the details.

state. Although the performance decreases as the number of CPU cores increases, it is around 30–40% up to 30720 cores (8 cores per node). The right panel of Fig. 4 shows the ratio to the peak performance as a function of the atomic numbers. The nuclear states listed in the figure are for the ground state of each nucleus. From the figure, the dependence of the performance on atomic number A is relatively weak for

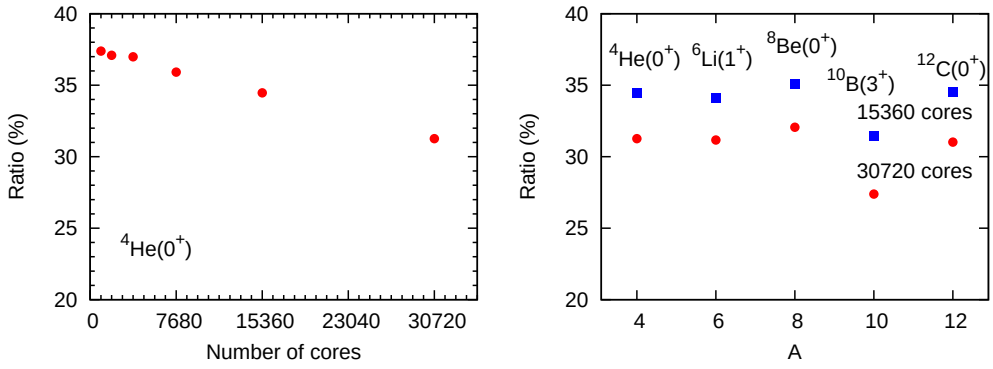

Figure 4: Ratio to the peak performance of the MCSM test calculations. Peak ratio of the calculation for the ^{4}He (0^+) ground state as a function of the number of cores (left). Peak ratio of the calculation for the ground states as a function of the number of nucleons (right). Red circles denotes the results with 30720 cores, and blue squares are with 15360 cores.

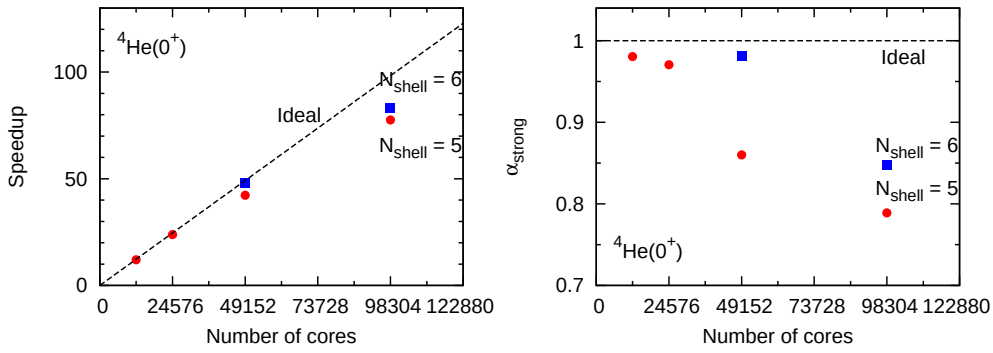

Figure 5: Speedup of the parallel computation with arbitrary unit (left), and the strong scaling (right).

the number of nucleons at least up to $A = 12$.

For testing the parallel efficiency, we have measured the dependence on the number of CPU cores. Figure 5 demonstrates the speedup (left) and the strong scaling (right) of our MCSM code on K computer as a function of the cores. The test case is the optimization of the 15th (48th) basis for ^{4}He (0^+) ground state in $N_{\rm shell} = 5$ (6) with 100 CG iterations without the preprocessing. Each setup has been chosen so that the number of MPI tasks is divisible by $N_{\rm procs}$, for simplicity. $32 \times 32 \times 30$ mesh points are used for the angular momentum projection, and 2 for the parity projection.

The left panel describes the speedup with arbitrary unit. In Fig. 5, the dotted line describes the perfect (ideal) scaling. The right panel of Fig. 5 is about the strong scaling. Here $\alpha_{\rm strong}$ is defined by the ratio of the time T with the number of CPU cores $N_{\rm procs}$ as $\alpha_{\rm strong} \equiv T(N_{\rm procs})/(T(N_{\rm procs}/2) \times 2)$. In this definition, $\alpha_{\rm strong} = 1$ describes the perfect strong scaling. As seen in Fig. 5, the strong scaling is nearly perfect up to 98304 cores both in $N_{\rm shell} = 5$ and 6.

3 Benchmarks

The recent development of the MCSM algorithm [7] , together with significant computational resources, enables us to perform a benchmark of no-core MCSM calculations [6]. Figure 6 is the recent comparison of the energies for each state and basis space in the selected p-shell nuclei between the MCSM and FCI methods. The FCI gives the exact energies in the finite basis spaces, while the MCSM provides approximate energies. Thus the comparisons between them show how well the MCSM works in no-core calculations. Furthermore, we also plot the No-Core Full Configuration (NCFC) [9] results for the states of $4 \leq A \leq 10$ as the fully converged energies in the infinite basis space.

For this benchmark comparison, the JISP16 two-nucleon interaction [10] is adopted and the Coulomb force is turned off. The energies are evaluated for the optimal harmonic oscillator frequencies where the calculated energies are minimized for each state and basis space. Here the contributions from the spurious center-of-mass motion are ignored for simplicity. The basis space ranges from $N_{\rm shell} = 2$ to 5 where $N_{\rm shell}$ is the number of the major shell included in the basis space. Some energies in $N_{\rm shell} = 4$ and 5 are available only from the MCSM results, as the M-scheme dimensions for these states are already close to or above the current computational limitation in the FCI approach. We took 100 importance-truncated basis states and extrapolated the results by the energy variance.

As seen in Fig. 6, the energies are consistent with each other to within ~ 100 keV where both results are available. Furthermore the $N_{\rm shell} = 5$ results begin to show

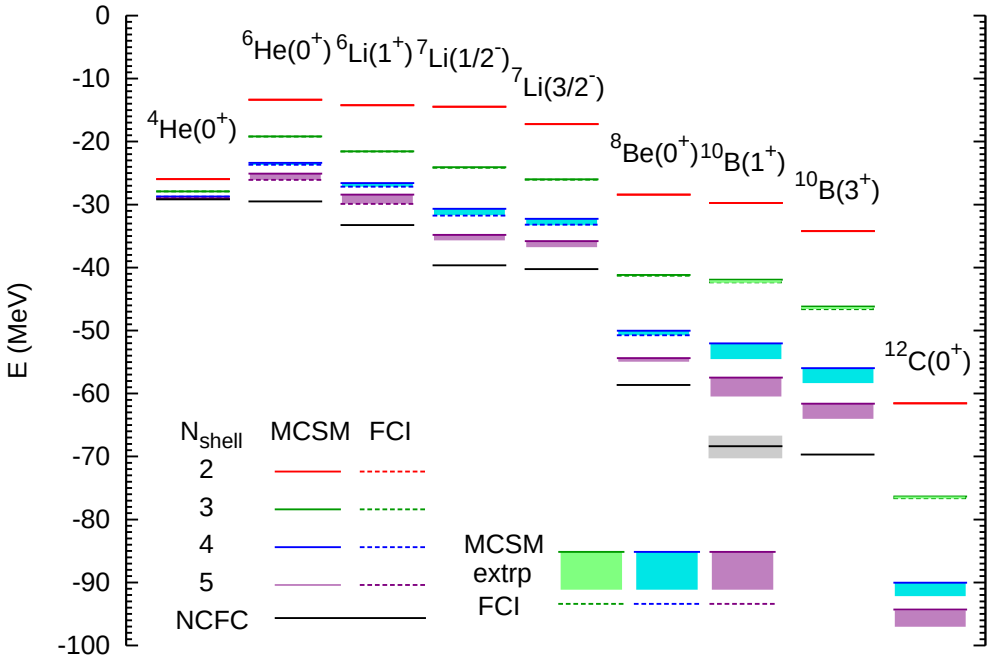

Figure 6: Comparisons of the energies between the MCSM and FCI along with the fully converged NCFC results where available. The NCFC result for the ^{10}B(1^+) state has a large uncertainty indicated by the grey band. The MCSM (FCI) results are shown as the solid (dashed) lines that nearly coincide where both are available. The extrapolated MCSM results are illustrated by bands. From top to bottom, the truncation of the basis space is $N_{\rm shell} = 2$ (red), 3 (green), 4 (blue), and 5 (purple). Note that the MCSM results are extrapolated by the energy variance with the second-order polynomials. Also note that the FCI results in $N_{\rm shell} = 2$ (red dotted lines) and 3 (green dotted lines) are almost overlapped with the MCSM results (red and green solid lines), which means that the MCSM results are converged well to the FCI results. Some results in $N_{\rm shell} = 4$ and 5 were obtained only with MCSM.

the trend of the convergence to the NCFC results obtained by extrapolating the $N_{\rm max}$ truncated results to the infinite basis space. The next step is to extrapolate the $N_{\rm shell}$ results to the infinite basis space by using the extrapolation techniques in the $N_{\rm max}$ truncation [9, 11, 12]. In principle, the results extrapolated to the infinite basis space should be consistent with each other in spite of how the basis spaces are truncated. It is interesting to examine whether the extrapolated results in the $N_{\rm shell}$ and $N_{\rm max}$ truncations converge to the same value within quantified uncertainties. The detailed comparisons among the MCSM, FCI, and NCFC methods are discussed in Ref. [6].

4 Summary

By exploiting the recent development in the MCSM algorithm, no-core calculations with the MCSM algorithm can be achieved on massively parallel supercomputers. As a test on such environments, we have discussed the performance of the MCSM on the K computer. From the benchmark calculations, the observables give good agreement between the MCSM and FCI results in the p-shell nuclei. The $N_{\rm shell} = 5$ results reveal the onset of systematic convergence pattern. Further work is needed to investigate the extrapolation to the infinite basis space in the $N_{\rm shell}$ truncation.

Acknowledgments

This work was supported in part by the SPIRE Field 5 from MEXT, Japan. We also acknowledge Grants-in-Aid for Young Scientists (Nos. 20740127 and 21740204), for Scientific Research (Nos. 20244022 and 23244049), and for Scientific Research on Innovative Areas (No. 20105003) from JSPS, and the CNS-RIKEN joint project for large-scale nuclear structure calculations. This work was also supported in part by the US DOE Grants No. DESC0008485 (SciDAC-3/NUCLEI), and DE-FG02-87ER40371, by US NSF Grant No. PHY-0904782, and through JUSTIPEN under grant No. DE-FG02-06ER41407. A part of the MCSM calculations was performed on the K computer at AICS, the T2K Open Supercomputer at the University of Tokyo and University of Tsukuba, and the BX900 Supercomputer at JAEA. Computational resources for the FCI and NCFC calculations were provided by the National Energy Research Supercomputer Center (NERSC), which is supported by the Office of Science of the U.S. Department of Energy under Contract No. DE-AC02-05CH11231, and by the Oak Ridge Leadership Computing Facility at the Oak Ridge National Laboratory, which is supported by the Office of Science of the U.S. Department of Energy under Contract No. DE-AC05-00OR22725.

References

[1] For a recent review, see, e. g., W. Leidemann and G. Orlandini, Progr. Part. Nucl. Phys. **68**, 158 (2013).

[2] P. Navrátil, J. P. Vary and B. R. Barrett, Phys. Rev. Lett. **84**, 5728 (2000); Phys. Rev. C **62**, 054311 (2000); S. Quaglioni and P. Navrátil, Phys. Rev. Lett. **101**, 092501 (2008); Phys. Rev. C **79**, 044606 (2009). For a recent review, see, e. g., B. R. Barrett, P. Navratil and J. P. Vary, Progr. Part. Nucl. Phys. **69**, 131 (2013).

[3] R. Roth and P. Navrátil, Phys. Rev. Lett. **99**, 092501 (2007); R. Roth, Phys. Rev. C **79** 064324 (2009); R. Roth, J. Langhammer, A. Calci, S. Binder and P. Navrátil, Phys. Rev. Lett. **107**, 072501 (2011); R. Roth, S. Binder, K. Vobig, A. Calci, J. Langhammer and P. Navrátil, *ibid.* **109**, 052501 (2012).

[4] T. Dytrych, K. D. Sviratcheva, C. Bahri, J. P. Draayer and J. P. Vary, Phys. Rev. Lett. **98**, 162503 (2007); Phys. Rev. C **76**, 014315 (2007); J. Phys. G **35**, 095101 (2008). For a review, see T. Dytrych, K. D. Sviratcheva, J. P. Draayer, C. Bahri and J. P. Vary, *ibid.* **35**, 123101 (2008).

[5] L. Liu, T. Otsuka, N. Shimizu, Y. Utsuno and R. Roth, Phys. Rev. C **86**, 014304 (2012).

[6] T. Abe, P. Maris, T. Otsuka, N. Shimizu, Y. Utsuno and J. P. Vary, Phys. Rev. C **86**, 054301 (2012).

[7] N. Shimizu, Y. Utsuno, T. Mizusaki, T. Otsuka, T. Abe and M. Honma, Phys. Rev. C **82**, 061305(R) (2010); N. Shimizu, Y. Utsuno, T. Mizusaki, M. Honma, Y. Tsunoda and T. Otsuka, *ibid.* **85**, 054301 (2012); Y. Utsuno, N. Shimizu, T. Otsuka and T. Abe, Comput. Phys. Commun. **184**, 102 (2013); N. Shimizu, T. Abe, Y. Tsunoda, Y. Utsuno, T. Yoshida, T. Mizusaki, M. Honma and T. Otsuka, Progr. Theor. Exp. Phys. 01A205 (2012).

[8] M. Honma, T. Mizusaki and T. Otsuka, Phys. Rev. Lett. **75**, 1284 (1995); **77**, 3315 (1996); T. Otsuka, M. Honma and T. Mizusaki, *ibid.* **81**, 1588 (1998), For a review, see T. Otsuka, M. Honma, T. Mizusaki, N. Shimizu and Y. Utsuno, Progr. Part. Nucl. Phys. **47**, 319 (2001).

[9] P. Maris, J. P. Vary and A. M. Shirokov, Phys. Rev. C **79**, 14308 (2009); P. Maris, A. M. Shirokov and J. P. Vary, *ibid.* **81**, 021301 (2010); C. Cockrell, J. P. Vary and P. Maris, *ibid.* **86**, 034325 (2012).

[10] A. M. Shirokov, J. P. Vary, A. I. Mazur and T. A. Weber, Phys. Lett. B **644**, 33 (2007); A. M. Shirokov, J. P. Vary, A. I. Mazur, S. A. Zaytsev and T. A. Weber, *ibid.* **621**, 96 (2005).

[11] R. J. Furnstahl, G. Hagen and T. Papenbrock, Phys. Rev. C **86**, 031301 (2012); S. N. More, A. Ekstrom, R. J. Furnstahl, G. Hagen and T. Papenbrock, *ibid.* **87**, 044326 (2013).

[12] S. A. Coon, M. I. Avetian, M. K. G. Kruse, U. van Kolck, P. Maris and J. P. Vary, Phys. Rev. C **86**, 054002 (2012); S. A. Coon, in *Proc. Int. Workshop Nucl. Theor. Supercomputing Era (NTSE-2012), Khabarovsk, Russia, June 18–22, 2012*, eds. A. M. Shirokov and A. I. Mazur. Pacific National University, Khabarovsk, 2013, p. 171, arXiv:1303.6358 [nucl-th] (2013).